

EVALUATION OF BENDING AND SHEAR CAPACITIES OF HPFRCC MEMBERS TOWARD THE STRUCTURAL APPLICATION

Toshiyuki Kanakubo, Katsuyuki Shimizu

Department of Engineering Mechanics and Energy, University of Tsukuba, Japan

Tetsushi Kanda, Satoru Nagai

Kajima Technical Research Institute, Japan

ABSTRACT

This paper describes the outline of the first building structure applied Reinforced ECC (Engineered Cementitious Composite) coupling beams and the quality assurance system by bending test for this actual application. To have knowledge for evaluation of performance of ECC members, the loading test for beam specimens is conducted with ECC tensile evaluation tests involving uniaxial tension test and bending test. From the test results, the conversion factors for tensile strength and ultimate tensile strain of ECC between uniaxial tension test and bending test are investigated. The evaluation methods for bending and shear strength of R/ECC beams are proposed using these material test results.

Keywords: Engineered Cementitious Composite, Uniaxial tension test, Bending test, Tensile strength, Ultimate tensile strain, Beam

1 INTRODUCTION

High Performance Fiber-Reinforced Cementitious Composites (HPFRCC), which show a strain hardening branch and multiple cracking under uniaxial tensile stress, have been focused by lots of researchers because of its unique mechanical performance. Engineered Cementitious Composites (ECC), which are introduced by Li [1], exhibit a maximum tensile strain of several percent owing to the synergetic effect of high-performance fiber and specifically designed mortar matrix. Unprecedented high-performance structural members can be expected when ECC is applied to seismic components.

The large numbers of worldwide studies on ECC presented so far have been limited to laboratory scale without experiences in full-scale plants. In 2005, however, reinforced ECC structural elements (R/ECC elements, hereafter) were first applied in building structure [2]. This application utilized R/ECC in a coupling beam connecting two structural walls in a 27-story high-rise RC building. The coupling beam is expected to have large deformation capacity and energy absorption performance under the seismic load. In addition to these mechanical properties, it is expected that high restoration performance due to multiple cracking leads sustainable building systems after the huge earthquake.

To realize this building structure, it was investigated in the project that quality assurance of fresh and mechanical properties of ECC in the actual plant is highly reliable, and its tensile properties can be verified by some test methods. A statistical evaluation of tensile properties and knowledge of performance standards are indispensable to the design of ECC structural members. In these flows of utilizing ECC, however, tensile properties of ECC are held as a mortgage to have an enough performance in the element level. The tensile strength and tensile deformability of ECC has not been considered directly to the structural design of R/ECC elements because of lacks of knowledge of performance standards necessary for designing ECC members. There have been insufficient discussions on how to refer to the design standard on tensile properties or how to evaluate structural performance of ECC members with keeping advantages to use ECC. These problems have been the obstacle to spread the usage of ECC in practical applications and needed to be quickly resolved.

This paper describes the outline of the first building structure applied R/ECC coupling beams and the quality assurance system by bending test for this actual application. To have knowledge for evaluation of performance of ECC members, we have conducted the loading test for beam specimens.

ECC tensile evaluation tests involving both uniaxial tension test and bending test, which was applied to the actual application, were carried out together for all beam test. These test results are also reported in this paper. After that, evaluation methods for bending and shear strength of ECC members are discussed based on the test results.

2 ACTUAL BUILDING CONSTRUCTION PROJECT USING ECC

2.1 Outline of Application and Inspection of ECC

R/ECC elements were first applied in building structure as shown in Fig.1. This application utilized R/ECC in a coupling beam connecting two structural walls in a 27-story high-rise reinforced concrete building 93m high. The coupling beam was 500mm wide by 900mm deep in cross section, and 1650mm long. Structural features in this application are referred to the literature [3].

These elements were produced one piece per day, for which ECC was mixed with an Omni-mixer in the plant as shown in Fig.2. Production started in November 2004 and was completed in June 2005. Element products and specimens for inspection were steam cured as for the full scale production experiments, and then cured in a stock field for at least 56 days.

The quality inspection process was determined as shown in Table 1, where lower bounds of tensile properties were adopted at 2MPa for strength and 0.5% for ultimate strain. For compressive strength, lower bound of 36 MPa, which is required from necessity in structural design, was adopted.

Tensile properties were inspected by bending test specified by JCI-S-003-2005. In the project, both uniaxial tension test shown in Fig.3 and bending test by 4 point loading shown in Fig.4 were executed to confirm mechanical properties of ECC. The adopted test method for uniaxial tension test has been introduced by authors [4]. This tensile specimen is used to minimize the influence of fiber orientation and is expected to reproduce a more precise tensile performance of ECC in a large size of members. Sectional dimension in test region is 100 x 60mm rectangle, which is 5 times larger than fiber length. Support conditions are one of the important factors for conducting uniaxial tension test for cementitious materials. In actual loading, it is impossible to perform "pure tension" because of the non-uniformity of the material itself and variations in specimen shapes and setup conditions. The "pin-fix" ends condition is selected as the better way to decrease the effect of eccentricity moment of tensile load and secondary moment after cracking [5]. Comparisons with uniaxial tension test results performed by other test methods can be found on the literature [5].

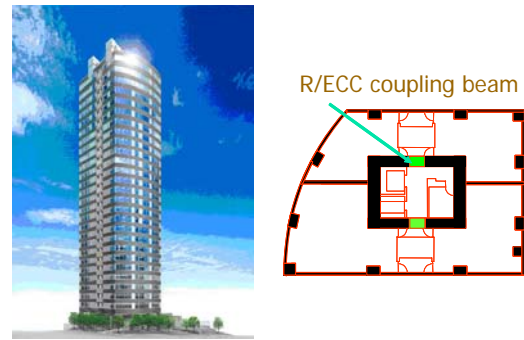


Fig.1 Application of ECC coupling beam



Fig.2 Omni mixer in actual plant

Table 1 Inspection outline for ECC

Property	Inspection	Testing specification	Frequency	Judgement for approval
Fresh	Slump flow	JIS A 1150	Once a day or once for each 150m ³ placing	530±100mm
	Air content	JIS A 1128		9±4%
	Fresh temperature	-		Over 5 less than 40 deg.
Mechanical	Compressive strength	JIS A 1108		Over 36MPa at 56day age
	Tensile strength	JCI-S-003-2005		Over 2MPa at 56day age
	Ultimate tensile strain			Over 0.5% at 56day age

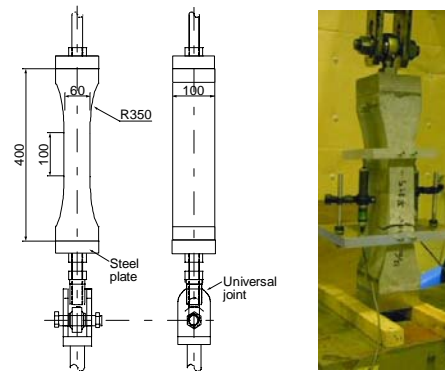


Fig.3 Uniaxial tension test

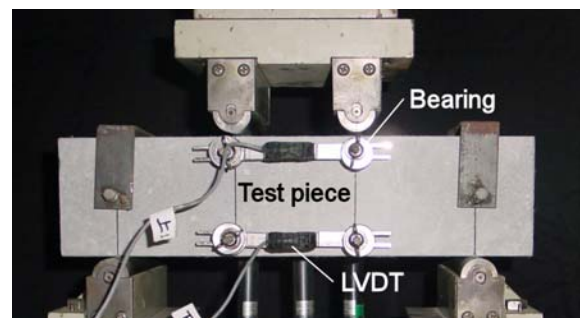


Fig.4 Bending test (JCI-S-003-2005)

The uniaxial tension test shown in Fig.3 requires a larger specimen and hence longer preparation time makes it difficult to adapt to a quality control routine test in the production of ECC components. The possible quality control method is the bending test, which is more realistic than uniaxial tension test. For the ultimate tensile strain and tensile strength, bending test data analyzed by using JCI-S-003-2005 Appendix are compared with those of the uniaxial tension test in Fig.5. It is shown that both ultimate tensile strain and tensile strength of ECC can be evaluated on the safe side by multiplying by a conversion factor of 0.7 on the basis of bending test

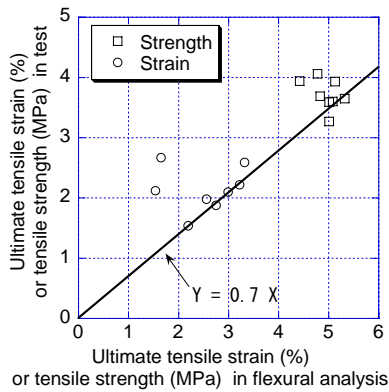


Fig.5 Tensile strength and ultimate tensile strain correlation between tensile test and bending test

and associated analysis. Taking into account the ease of execution and simplicity of the apparatus, the bending test may be the most realistic solution for quality control. Tensile properties of ECC were inspected by bending test and the results in Fig.5 are reflected in the inspection process shown in Table 1.

2.2 Results of Inspection of ECC

In the actual processing, all inspection items were satisfied. The results of fresh property inspection and mechanical property inspection are depicted in Fig.6, where all fresh inspection data and all mechanical data satisfied the specification in Table 1. In the 58 days of production, the lowest magnitudes were: 36.3 MPa in compressive strength, 2.37 MPa in tensile strength, and 0.59% in ultimate tensile strain.

3 LOADING TEST ON BEAM SPECIMEN

As described in Chapter 1, tensile properties of ECC are held as a mortgage to have an enough performance in the element level in the previous introduced application. The tensile strength and tensile deformability of ECC has not been considered directly to the structural design of R/ECC elements. In this chapter, bending shear test results for beam specimens are reported in order to complement lacks of knowledge of performance

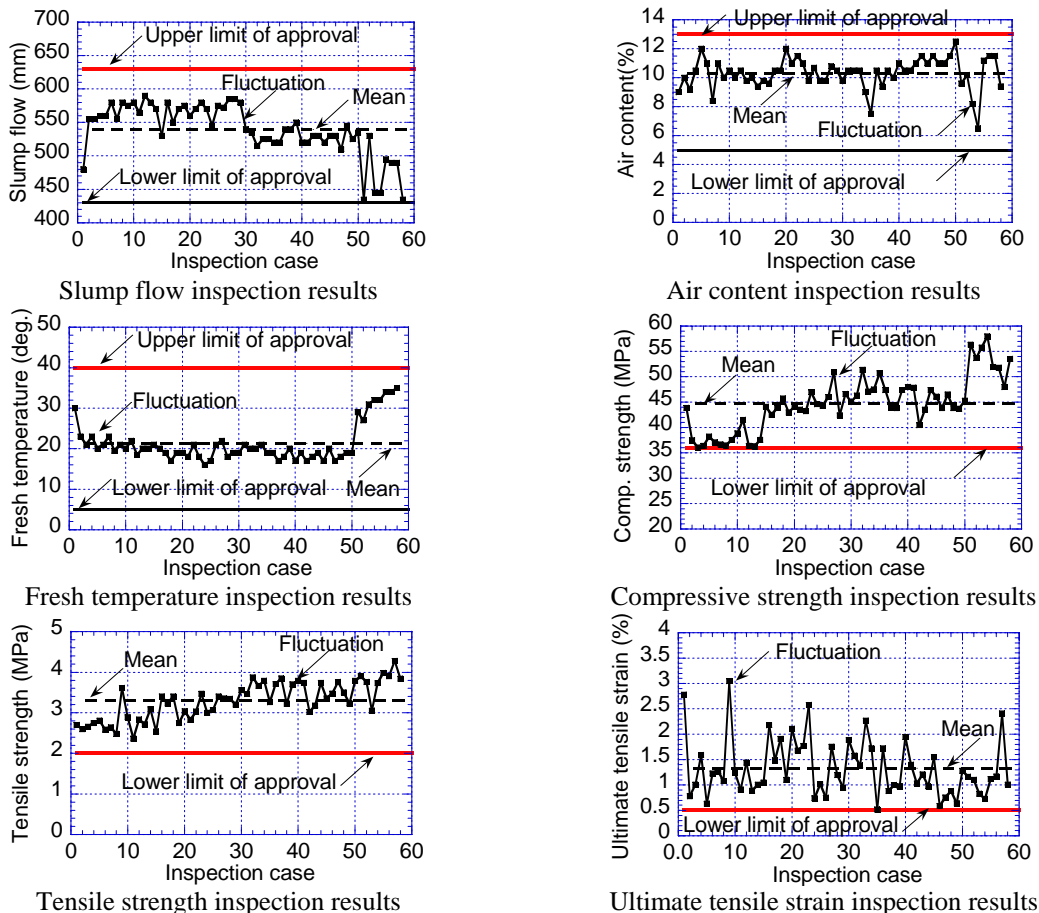


Fig.6 Results of inspection of ECC properties

standards necessary for designing ECC members. The results of tensile property evaluation tests involving uniaxial tension and bending test are also discussed in this chapter.

3.1 Used Materials for ECC

PVA fiber shown in Table 2 was utilized in the experimental program. These values are given by manufacturer. Mix proportions are summarized in Table 3. Fiber volume fraction was set to 1.5 and 2%. Compressive strength at the testing age ranges from 35.7 to 50.3MPa by using 100 ϕ -200mm cylinder test piece. Hereafter, ECC with 1.5% and 2.0% PVA fiber volume fraction is identified as PVA15 and PVA20, respectively.

Table 2 Properties of PVA fiber

Fiber type	Fiber length (mm)	Diameter (mm)	Tensile strength (MPa)	Elastic modulus (GPa)
PVA	12	0.04	1600	40

Table 3 Mix proportion of PVA-ECC

Water by binder ratio	Sand by binder ratio	Air content (%)	Fiber vol. fraction (%)
0.42	0.77	10	1.5, 2.0

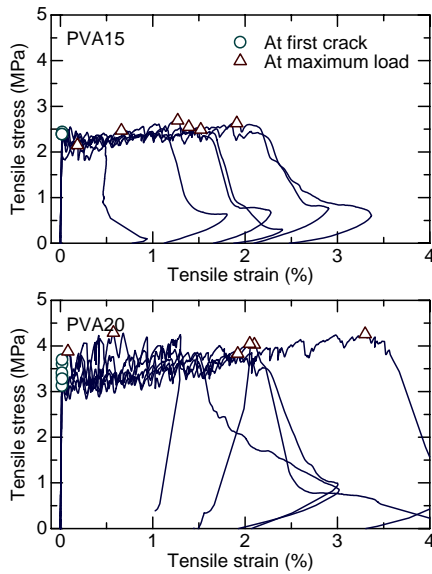


Fig.7 Uniaxial tension test result

3.2 Tensile Property Evaluation

Uniaxial tension test shown in Fig.3 and bending test shown in Fig.4 were executed. Examples of tensile stress – tensile strain curves and bending moment – curvature curves are shown in Fig.7 and Fig.8, respectively. Tensile strain in uniaxial tension test is calculated that elongation measured by LVDTs is divided by gauge length of 160mm. Curvature in bending test is calculated as the slope of strains obtained by LVDTs set on the compression and tension side.

Both PVA15 and PVA20 shows pseudo strain hardening behavior in tension, and deflection hardening behavior in bending. We had a total of 11 batches for PVA20 and 2 batches for PVA15 specimens combinations. All test results are summarized in Table 4. From 3 to 6 specimens were tested in each batch and the results are average values. Tensile strength of PVA20 and PVA15 obtained by uniaxial tension test is 3.7MPa and 3.3MPa as average values, respectively. Ultimate tensile strain, which is defined that the point where stress begins to decrease continuously with increase

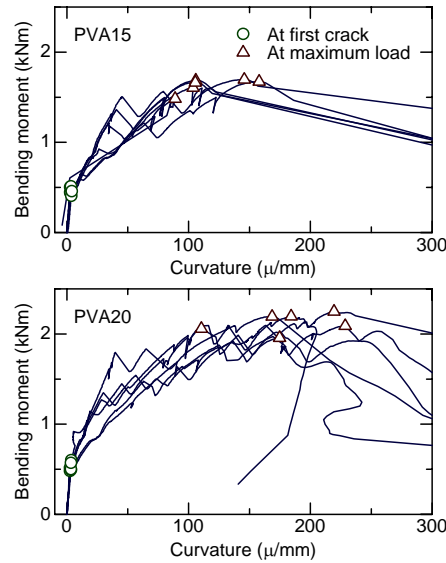


Fig.8 Bending test result

Table 4 Test results and evaluation values by bending test

ID Batch No.	Uniaxial tension test		Bending test				
	Ultimate tensile strain (%)	Tensile strength (MPa)	Curvature at max. (1/m)	Maximum moment (kNm)	Evaluation method		
					Ultimate tensile Strain (%)	Tensile strength (MPa)	
PVA20	No.1	1.19	3.37	0.201	2.07	1.72	4.58
	No.2	1.66	4.05	0.145	2.03	1.21	4.57
	No.3	2.02	4.16	0.267	1.66	2.36	3.59
	No.4	1.63	2.87	0.174	1.33	1.49	3.01
	No.5	2.92	4.18	0.349	1.53	3.10	3.33
	No.6	2.13	4.06	0.183	2.11	1.53	4.75
	No.7	0.91	3.40	0.0839	1.86	0.67	4.33
	No.8	1.98	3.69	0.297	2.16	2.56	4.83
	No.9	2.10	3.60	0.344	2.30	2.99	5.07
	No.10	2.22	3.94	0.370	2.00	3.22	4.41
	No.11	2.59	3.27	0.382	2.25	3.32	4.97
PVA15	No.1	1.50	2.50	0.124	1.66	1.02	3.83
	No.2	0.64	2.99	0.0528	1.55	0.41	3.66

in strain, of PVA20 and PVA15 is 1.9% and 1.1%, respectively. The differences in strength and ultimate strain due to fiber volume fraction are recognized.

Evaluation method for tensile strength and ultimate tensile strain of fiber reinforced cementitious composites has been introduced as the appendix of JCI-S-003-2005. The evaluation method is introduced based on the following assumptions for stress distribution under the maximum bending moment as shown in Fig. 9.

- i) The stress distribution on the compression side is triangular.
- ii) The stress distribution on the tension side is uniform ($f_{t,b}$).

These assumptions represent a state in which the strain on the tension edge has reached the ultimate strain ($\epsilon_{tu,b}$) but the stress on the compression edge has not reached the compressive strength under the maximum bending moment. It is considered that these assumptions generally agree with actual strain and stress distributions of ECC.

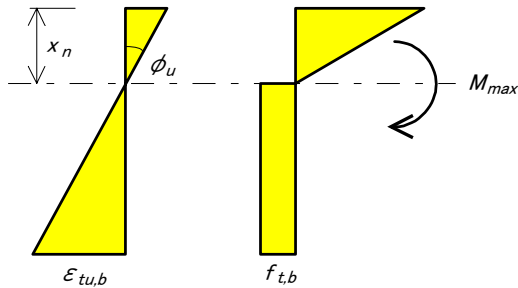


Fig.9 Stress distribution assumption (JCI-S-003-2005)

Table 4 also includes the evaluation values for tensile strength and ultimate tensile strain by JCI-S-003-2005 Appendix method. Tensile strength of PVA20 and PVA15 evaluated by this method is 4.3MPa and 4.0MPa as average values, respectively. Ultimate tensile strain of PVA20 and PVA15 is 2.2%

and 0.7%, respectively. Fig.10 shows the comparisons of tensile strength and ultimate tensile strain between obtained values by uniaxial tension test and evaluated value by bending test. From the regression analysis, ultimate tensile strain and tensile strength of uniaxial test is 0.85 and 0.82 of those of bending test, respectively. Both values can be evaluated on the safe side by multiplying by a conversion factor of 0.7 as same as Fig.5.

It is important to note that these conversion factors may vary according to the material properties, size of the bending test specimen and loading conditions. This dependency originates from the fact that bending performance is a structural performance strongly sensitive to specimen size and loading conditions while tensile performance by nature can be regarded as a material property. Thus, the prediction of tensile performance by means of a bending test should be executed with special care of the targeted materials, and the conversion factors may vary depending on the bending test conditions. At the present technical levels, the conversion factors may not be derived theoretically and may be reasonably treated as experimental parameters.

A brief remark based on mechanics is presented as follows. The difference on ultimate tensile strain between tension test and bending test reflects easier multiple crack formation under bending than under tension. When the ultimate bending load exceeds the initial cracking load during bending, an increase in flexural deflection is accompanied by multiple fine cracking between the loads. This phenomenon is known as deflection hardening, which is demonstrated in Fig.8. Deflection hardening, although it looks similar to strain hardening under tension as shown in Fig.7, occurs under milder mechanical conditions than strain hardening. A straightforward example is the analytical consequence by Naaman [6] that, when compressive strength is high enough, the tensile strength of a

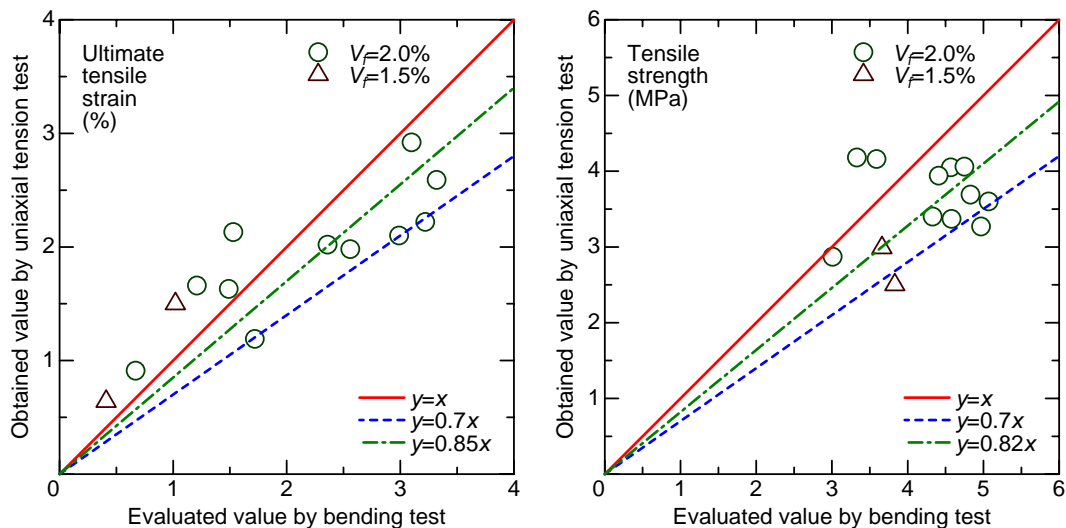


Fig.10 Comparisons of tensile properties between uniaxial tension test and bending test evaluation

composite necessary to show deflection hardening is one third of the strength of matrix cracking. When strain hardening occurs under tensile loading, the tensile strength of the composite material should be greater than the matrix cracking strength. It is important to note the difference between deflection and strain hardening since multiple cracking occurs more easily under bending than under tensile loading. The difference on ultimate tensile strain between tension test and bending test representing the difference in conditions of multiple crack formation in bending or in tension has a meaning that reduces the ultimate strain predicted from a bending test.

The other difference on tensile strength between tension test and bending test represents the difference between tensile stress – strain relations assuming perfect elasto-plasticity in Fig.9 and reality. As can be seen from Fig.7, the stress-strain relation of ECC can in general be approximated as bi-linear where stress increases gradually after initial cracking. The predicted tensile strength is based on the perfect elasto-plastic model and is likely to be greater than that obtained in the uniaxial tension test (JCI-S-003-

2005 Appendix), and an error that may be involved in the assumptions of the stress-strain relation forms.

3.3 Bending Shear Test on Beam Specimen (1) Specimen and loading method

The dimensions and reinforcing bar arrangements of the beam specimens are shown in Fig.11 and list of specimens are shown in Table 5. Specimens have the 180 x 280mm size rectangular section, and shear span ratio (M/QD) is 1.5 (L specimen) and 1.25 (S specimen). Arrangements of main bars and stirrups are D13 and D4 or D6 stirrup. Parameters are PVA fiber volume fraction (V_f), shear span ratio, ratio of stirrup (p_w) and yield strength of main bar (σ_y). Fiber volume fraction of PVA fiber was set to 1.5 or 2.0%. Beam specimens named by the last alphabet of F are designed to have flexural yielding before failure. Other specimens are designed to show shear failure before flexural yielding.

Loading was carried out by Ohno method under anti-symmetrical moment with monotonic manner. LVDTs were set to measure relative displacement

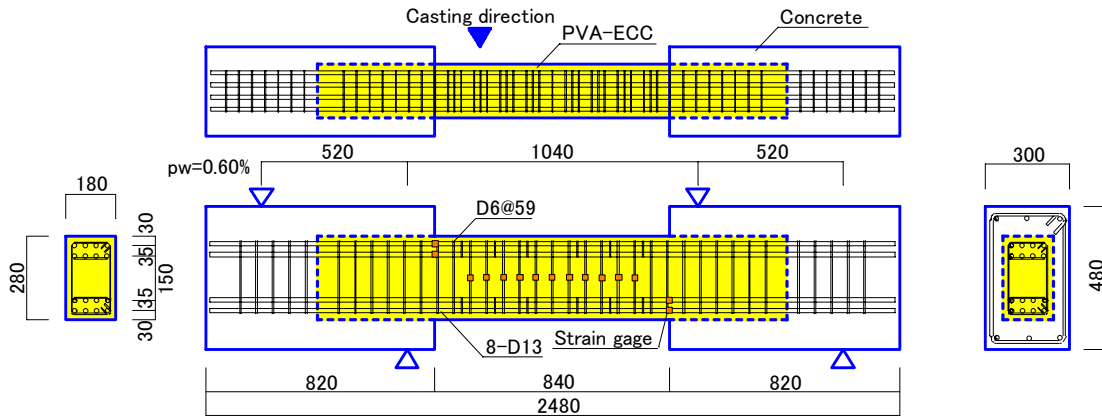


Fig.11 Example of beam specimen arrangement (PVA20-60L)

Table 5 List of beam specimen

Identification	V_f (%)	M/QD	L (mm)	$b \times D$ (mm)	Main Bar		Stirrup					
					Arrangement	σ_y (MPa)	Arrangement	p_w (%)	σ_{wy} (MPa)			
PVA15-00L	1.5	1.50	840	180 x 280	8-D13 $p_f=2.43\%$	719	-	0.00	-			
PVA15-15L							2-D4@93	0.15	295			
PVA15-30L							2-D4@47	0.30				
PVA15-60L						711	2-D6@59	0.60	334			
PVA15-89L							438	2-D6@40		0.89		
PVA15-89LF									691		4-D6@59	1.20
PVA15-89S		1.25	700			700	700	691	-	0.00	-	
PVA15-120S									719	2-D4@93	0.15	295
PVA20-00L										2-D4@47	0.30	
PVA20-15L	2.0	1.50	840	180 x 280	8-D13 $p_f=2.43\%$	711	2-D6@59	0.60	334			
PVA20-30L							438	2-D6@40		0.89		
PVA20-60L									691		4-D6@59	1.20
PVA20-89L		1.25	700			700	700	691	-	0.00	-	
PVA20-89LF									719	2-D4@93	0.15	295
PVA20-89S										2-D4@47	0.30	
PVA20-120S	711	2-D6@59	0.60	334								
PVA20-89L		438	2-D6@40		0.89							
PVA20-89LF	691			4-D6@59		1.20	427					

between the stubs. Strain gauges were set to measure main bar and stirrup strain.

(2) Material test for PVA-ECC

Compression test using 100φ-200mm cylinder test piece and bending test by JCI-S-003-2005 was executed. The test results are shown in Table 6. Tensile strength and ultimate tensile strain obtained by JCI-S-003-2005 Appendix method is multiplied by 0.82 and 0.85, respectively, based on the discussion in Section 3.2.

(3) Test results

Beam specimens after loading are shown in Fig.12, and shear force – translational angle curves are shown in Fig.13. Bending and shear crack are observed at 0.0025rad. The multiple cracks and restrain effect of crack opening could be observed. In beam specimens of shear failure type, when load becomes around the maximum value, deformation was concentrated on a certain one shear crack. The width of other cracks decreased due to localized

Table 6 Material test results of PVA-ECC

Type	Compression test			Bending test ^{*1}		Specimen for
	Elastic modulus (GPa)	Compressive strength (MPa)	Strain at strength (%)	Tensile strength (MPa)	Ultimate tensile strain (%)	
PVA20	19.5	39.1	0.36	3.90	1.30	$p_w=0.00 - 0.30\%$ L
	19.5	45.8	0.39	3.55	0.57	$p_w=0.60 - 0.89\%$ L
	19.9	44.3	0.48	3.93	0.91	$p_w=0.89 - 1.20\%$ S
PVA15	16.3	35.7	0.35	3.14	0.87	$p_w=0.00 - 0.30\%$ L
	19.4	50.3	0.39	3.00	0.35	$p_w=0.60 - 0.89\%$ L
	17.4	42.0	0.42	1.98	0.36	$p_w=0.89 - 1.20\%$ S

*1 Obtained by JCI-S-003-2005 Appendix method multiplied by 0.82 for tensile strength and 0.85 for ultimate tensile strain

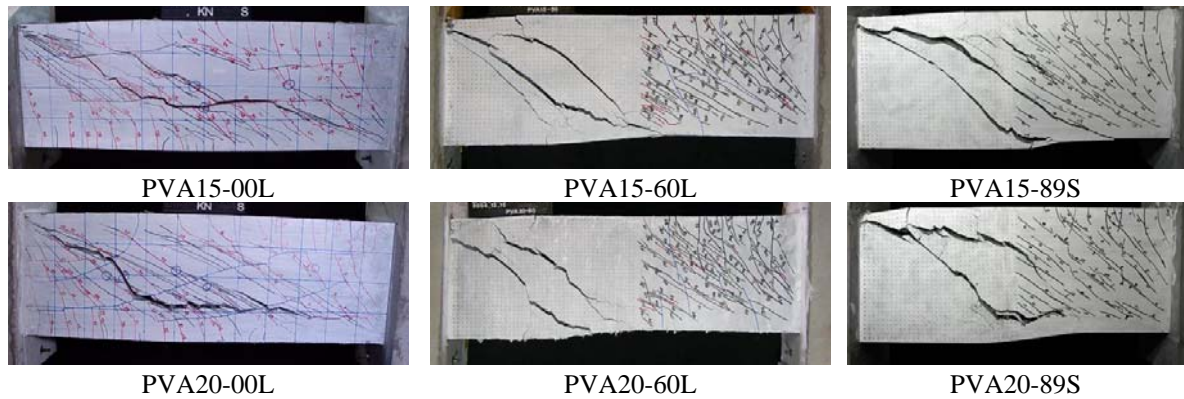


Fig.12 Failure pattern after loading

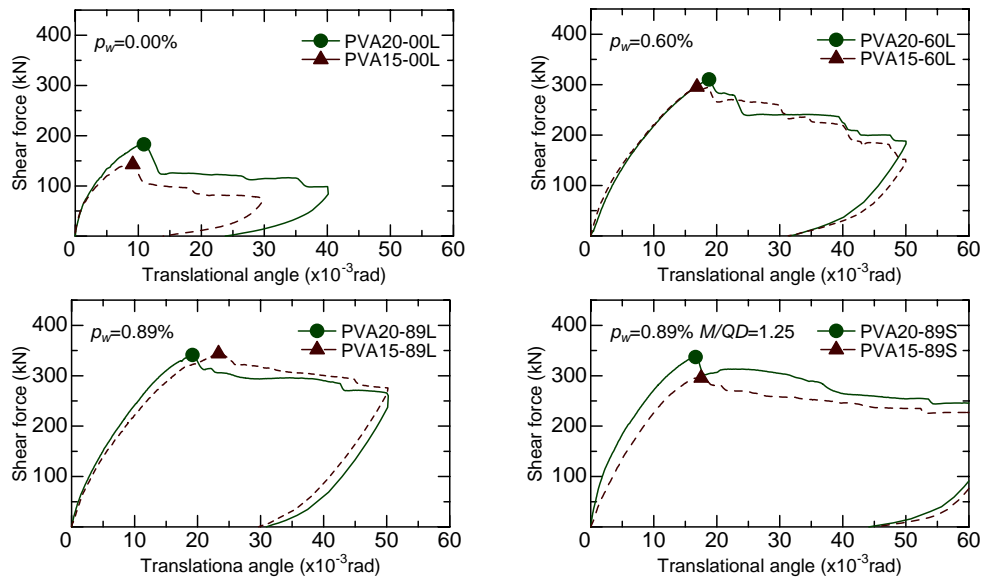


Fig.13 Shear force – translational angle curves

Table 7 Test results of beam specimen

Identification	Translational angle ($\times 10^{-3}$ rad) at		At maximum load		Ultimate angle ^{*1} ($\times 10^{-3}$ rad)	Failure Mode ^{*2}
	Stirrup yielding	Main bar yielding	Shear force (kN)	Trans. angle ($\times 10^{-3}$ rad)		
PVA15-00L	-	-	143	8.7	10.4	S
PVA15-15L	2.60	-	170	15.0	17.9	S
PVA15-30L	3.27	-	183	12.0	14.3	S
PVA15-60L	8.34	-	296	16.9	31.1	S
PVA15-89L	11.8	22.7	344	23.3	>50	F -> S
PVA15-89LF	13.1	10.8	270 ^{*3}	>50 ^{*3}	>50	F
PVA15-89S	8.36	-	296	17.5	46.0	S
PVA15-120S	7.34	-	344	22.0	56.1	S
PVA20-00L	-	-	183	10.6	12.6	S
PVA20-15L	-	-	206	12.8	15.2	S
PVA20-30L	5.50	-	209	19.0	22.6	S
PVA20-60L	11.1	-	310	18.8	23.9	S
PVA20-89L	11.5	19.2	341	19.2	43.1	F -> S
PVA20-89LF	11.6	10.8	272 ^{*3}	>50 ^{*3}	>50	F
PVA20-89S	9.43	-	337	16.6	38.6	S
PVA20-120S	9.23	19.7	409	23.9	44.9	F -> S

*1 : Translational angle when load decreases to 80% of Maximum *2 : S=Shear failure, F=Flexural yielding
 *3 : At the last point for deloading (1/20rad.)

deformation. The large difference between PVA15 and PVA20 specimen could not be recognized. In PVA15-89LF and PVA20-89LF specimens, load is in process of increasing when translational angle becomes 0.05rad.

Test results are summarized in Table 7. Maximum load and translational angle at maximum load increase as fiber volume fraction and stirrup ratio also increases.

4 EVALUATION OF BENDING AND SHEAR STRENGTH OF BEAM SPECIMEN

To complement the lacks of knowledge of performance standards necessary for designing ECC members, we would like to propose evaluation methods for bending and shear strength of R/ECC members based on the test results. Material properties are most important in evaluating member structural performance. In this paper, material properties for tension of ECC have been cleared by both uniaxial test and bending test. In this chapter, evaluated value by JCI-S-003-2005 Appendix method is adopted as tensile strength and ultimate tensile strain of ECC. The conversion factors of 0.82 for tensile strength and 0.85 for ultimate tensile strain is multiplied to these evaluated values.

4.1 Bending Strength

Bending strength is calculated by fiber analysis under the assumption that plane section remains plain. This basis is as same as the case of ordinary reinforced concrete. The tensile stress of ECC is considered by representing model of tensile stress – tensile strain relations of ECC as perfect elasto-

plasticity model. The ultimate tensile strain (ϵ_u) of the model is given by $0.85\epsilon_{tu,b}$ and tensile strength (σ_t) of the model is given by $0.82f_{t,b}$. Compressive stress – strain relation is modeled by parabolic curves referring to the compression test results. These models are shown in Fig.14. Elastic modulus for tension side is regarded as same as the elastic modulus obtained by compression test (cE).

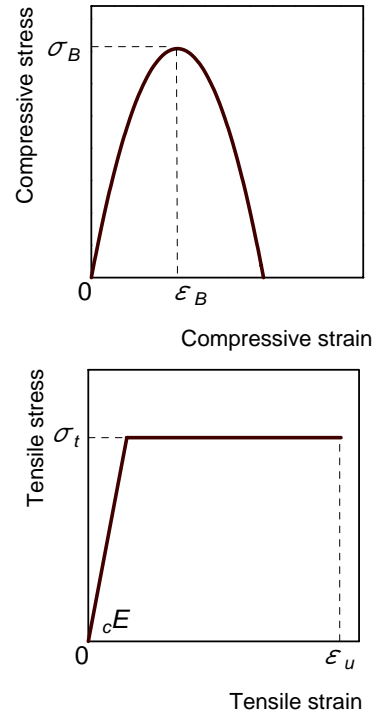


Fig.14 Stress – strain models for fiber analysis.

4.2 Shear Strength

It is assumed that principal tensile stress of ECC keeps tensile strength (σ_t) at shear failure. The average of tensile stress on beam is expressed by σ_t with a reduction factor (ν_t). We considered that beam specimen exhibits the maximum load when compressive strut is failed by principal compressive stress as shown in Fig.15. As a matter of fact, compressive failure at crack zone of beam specimen was recognized as shown in Fig.16. Because the compressive strut has some angles with main shear crack, local compressive failure takes place at the crack surface. This approach has same way to ordinary RC beam. In case of RC, shear transmitting force at the crack surface is carried by mainly bearing of coarse aggregate. In case of R/ECC, the force is carried by bridging of fiber.

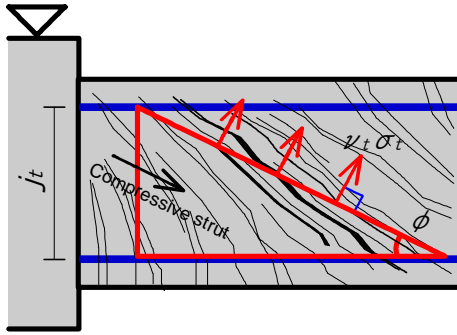


Fig.15 Model for shear strength

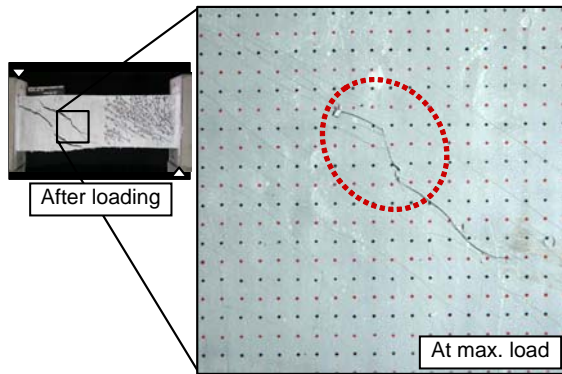


Fig.16 Local compression failure on beam

If we use AIJ A-Method [7] as a basic formula to express shear strength, shear strength of R/ECC beam is calculated as follows;

$$V = V_t + V_a + V_{ECC} \quad (1)$$

$$V_t = b \cdot j_t \cdot p_w \cdot \sigma_{wy} \cdot \cot \phi \quad (2)$$

$$V_a = \tan \theta \cdot (1 - \beta) \cdot \nu \cdot \sigma_B \cdot b \cdot D / 2 \quad (3)$$

$$\tan \theta = \sqrt{(L/D)^2 + 1} - (L/D) \quad (4)$$

$$\beta = (1 + \cot^2 \phi) \cdot p_w \cdot \sigma_{wy} / \nu \cdot \sigma_B \quad (5)$$

$$\nu = 1.70 \sigma_B^{-0.333} \quad (6)$$

$$\cot \phi = \min \begin{cases} 2.0 \\ j_t / (D \cdot \tan \theta) \\ \sqrt{\nu \cdot \sigma_B / (p_w \cdot \sigma_{wy})} - 1 \end{cases} \quad (7)$$

$$V_{ECC} = b \cdot j_t \cdot \nu_t \cdot \sigma_t \cdot \cot \phi \quad (8)$$

where,

V : shear strength

V_t : shear strength by truss mechanism

V_a : shear strength by arch mechanism

b : width of member

j_t : distance between compression and tension bars

p_w : stirrup ratio

σ_{wy} : yield strength of stirrup

σ_B : compressive strength of ECC

ϕ : angle of compressive strut

θ : angle of arch mechanism

ν : effective coefficient of compressive strength of ECC

D : depth of member

L : clear span length

ν_t : reduction factor for tensile strength of ECC

σ_t : tensile strength of ECC

In above formulas, effective coefficient of compressive strength of ECC (ν) is treated as same as case of ordinary concrete proposed by fib.

Reduction factor for tensile strength of ECC (ν_t) is unknown. We decided the value of ν_t by reverse calculation using test results of beam specimens. The result of reverse calculation is indicated in Table 8. The value ranges from 0.27 to 0.56. The tendency by any structural factor such as shear span ratio, stirrup ratio and fiber volume fraction can not be observed. The average for all specimens is 0.41.

Though the precise meaning of this reduction factor is unknown, the followings may be pointed

Table 8 Reverse calculation result for ν_t

Identification	ν_t
PVA15-00L	0.32
PVA15-15L	0.35
PVA15-30L	0.32
PVA15-60L	0.54
PVA15-89L	0.56
PVA15-89S	0.27
PVA15-120S	0.42
Average	0.40
PVA20-00L	0.40
PVA20-15L	0.41
PVA20-30L	0.34
PVA20-60L	0.54
PVA20-89L	0.49
PVA20-89S	0.28
PVA20-120S	0.44
Average	0.41

out.

- ECC may not carry constant tensile strength along the shear crack under complex bi-axial stress field.
- Superposition of each term for truss, arch and ECC mechanism is based on the plasticity theory. This may need some reductions for certain term.

4.3 Verification

The experimental value of maximum shear force in beam test is plotted with calculated shear strength in Fig.17. Both maximum shear force and calculated shear strength is standardized by calculated bending strength in shear force. The calculated values are estimated by former sections' methods. In spite of the constant value of v_s , experimental values show good agreement with calculated values.

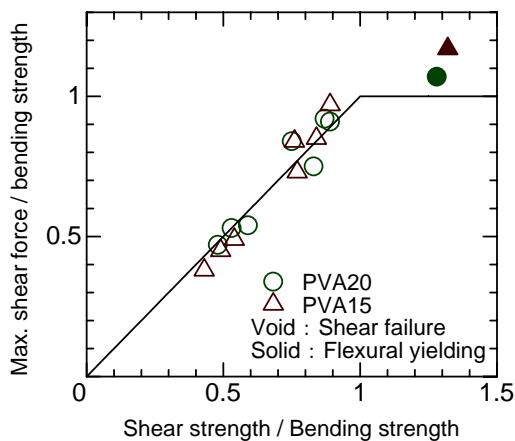


Fig.17 Comparison of calculated strength

5 SUMMARIES

This paper described the outline of the first building structure applied R/ECC coupling beams and the quality assurance system by bending test for this actual application. To have knowledge for evaluation of performance of ECC members, the loading test for beam specimens was conducted with ECC tensile evaluation tests involving both uniaxial tension test and bending test.

From the test results, the conversion factors for tensile strength and ultimate tensile strain of ECC between uniaxial tension test and bending test as the material properties were found out. The evaluation methods for bending and shear strength of R/ECC beams were proposed using these material test

results.

It is most important that structural performance of R/ECC members is evaluated and inspected by certain material properties. In the case of ordinary RC structure system, the compression test is the only one method considering structural design of RC members. In case of ECC and HPRCC, it is indispensable to evaluate and inspect tensile characteristics of material such as tensile strength, tensile deformation capacity, and so on. The one example using bending test by JCI-S-003-2005 was introduced in this paper for evaluation of the member strength.

REFERENCES

- [1] V.C. Li : From Micromechanics to Structural Engineering -the Design of Cementitious Composites for Civil Engineering Applications, JSCE J. of Struc. mechanics and Earthquake Engineering, 10(2), pp.37-48, 1993
- [2] T. Kanda, S. Tomoe, S. Nagai, M. Maruta, T. Kanakubo and K. Shimizu : Full Scale Processing Investigation for ECC Pre-Cast Structural Element, Journal of Asian Architecture and Building Engineering, Vol.5, No.2, pp.333-340, 2006.11
- [3] M. Maruta, et al. : New High-Rise RC Structure Using Pre-Cast ECC Coupling Beam, Concrete Journal, Vol.43, No.11, pp.18-26, 2005 (*in Japanese*)
- [4] K. Shimizu, T. Kanakubo, T. Kanda and S. Nagai : Shear Behavior of Steel Reinforced PVA-ECC Beams, 13th World Conference on Earthquake Engineering, Conference Proceedings DVD, Paper No. 704, 2004
- [5] T. Kanakubo : Tensile Characteristics Evaluation Method for Ductile Fiber-Reinforced Cementitious Composites, Journal of Advanced Concrete Technology, Vol.4, No.1, pp.3-17, 2006
- [6] A.E. Naaman : Toughness, Ductility, Surface Energy and Deflection-Hardening FRC Composites, Proceedings JCI International Workshop on Ductile Fiber Reinforced Cementitious Composites (DFRCC), pp.33-57, 2002
- [7] Architectural Institute of Japan : Design Guidelines for Earthquake Resistant Reinforced Concrete Buildings Based on Ultimate Strength Concept, pp.106-116, 1990